Bioorganic & Medicinal Chemistry xxx (2014) xxx–xxx

Contents lists available at ScienceDirect

Bioorganic & Medicinal Chemistry

journal homepage: www.elsevier.com/locate/bmc

Design and synthesis of novel 2-pyrazoline-1-ethanone derivatives as selective MAO inhibitors

Xu Tong [a], Rui Chen [a], Tong-Tian Zhang [a], Yan Han [a], Wen-Jian Tang [a,*], Xin-Hua Liu [a,b,*]

[a] School of Pharmacy, Anhui Medical University, Hefei 230032, PR China
[b] State Key Laboratory of Pharmaceutical Biotechnology, Nanjing University, Nanjing 210093, PR China

ARTICLE INFO

Article history:
Received 29 October 2014
Revised 2 December 2014
Accepted 7 December 2014
Available online xxxx

Keywords:
Monoamine oxidase
Pyrazoline
MAOIs
Molecular docking

ABSTRACT

Thirty seven novel 2-pyrazoline-1-ethanone derivatives were designed, synthesized and evaluated as selective hMAO inhibitors. Among them, compounds **7h** (IC_{50} = 2.40 μM) and **12c** (IC_{50} = 2.00 μM) exhibited best inhibitory activity and selectivity against hMAO-A, surpassing that of the positive control Clorgyline (IC_{50} = 2.76 μM). Based on selective activity of hMAO-A, SAR analysis showed that the order of N1 substituent contribution was bromo (**3**) > piperidinyl (**4**) > morpholinyl (**5**) > imidazolyl (**6**), and compounds with electron-withdrawing substituents (-F, -Cl) at C3 or C5 phenyl ring of 2-pyrazoline nucleus dedicated stronger MAO-A inhibitory activity. Molecular docking showed that compounds **7h** and **12c** were nicely bound to hMAO-A via two hydrogen bonds (SER209, GLU216), one Pi–Pi interaction and three hydrogen bonds (SER209, GLU216, TYR69), one Sigma–Pi interaction, respectively. In addition, the substituent at C3 position of 2-pyrazoline with the N1 acetyl has little effect on MAO-A inhibitory activity. These data support further studies to assess rational design of more efficiently selective hMAO inhibitors in the future.

1. Introduction

Monoamine oxidases (MAOs) are a family of amine oxidoreductases containing flavin that play an important role in the regulation and metabolism of several neurotransmitters, and their inhibitors (MAOIs) could be useful in the treatment of psychiatric and neurological diseases.[1,2] Two isoforms of MAO, namely MAO-A and MAO-B, have been identified based on their amino acid sequences, three-dimensional structures, substrate specificity, and inhibitor selectivity.[3–5] MAO-A has a higher affinity for serotonin and noradrenaline, while MAO-B preferentially deaminates phenylethylamine and benzylamine. Despite of these differences, dopamine and tyramine are common substrates for both isoforms. These properties determine the pharmacological interest of MAOIs. MAO-A inhibitors act as antidepressant and antianxiety agents, whereas MAO-B inhibitors are used alone or in combination to treat Alzheimer's and Parkinson's diseases.[6,7] http://en.wikipedia.org/wiki/Monoamine_oxidase Therefore, the researcher's interest in the rational design is to search for novel, selective and efficient MAO inhibitors.

The development of synthetic heterocyclic compounds as MAOIs progressed considerably during the past decade. Different families of heterocycles containing 2 or 4 nitrogen atoms have been used as scaffolds for synthesizing selective MAOIs, but the early period of MAOIs started with hydrazine derivatives. Pyrazole, pyrazoline, and pyrazolidine derivatives can be considered as a cyclic hydrazine moiety, which scaffold showed promising antidepressant and anticonvulsant properties as demonstrated by different and established animal models. Substituted pyrazolines, decorated with different functional groups, are important lead compounds endowed with a large amount of biological activities.[8–10] Moreover, due to the direct correlation with the recognized MAO inhibition, this scaffold was used to design selective inhibitory agents for MAO-A or MAO-B isoforms.[11–15]

Previous structure–activity relationships (SARs) analysis on pyrazoline scaffold showed that the carbonyl or thiocarbonyl group at N1, capable of increasing the positive charge on N1, was reported to be important for MAO inhibition. When introducing substituents in α-position of the N1 acetyl, these compounds showed antidepressant-like activity in mice.[9,16,17] However, major substituents of 2-pyrazoline nucleus were aromatic rigid molecules, thus we would incorporate a heterocyclic ring at the N1 position of 2-pyrazoline with flexibility to increase MAO inhibitory effects.[18]

* Corresponding authors. Tel./fax: +86 551 65161115.
E-mail addresses: ahmupharm@126.com (W.-J. Tang), xhliuhx@163.com (X.-H. Liu).

http://dx.doi.org/10.1016/j.bmc.2014.12.010
0968-0896/

Based on the X-ray crystal structure hMAO-A complex (2BXR.pdb), computer-generated docking molecular models of 2-pyrazoline-1-ethanone derivatives were analyzed, when the α-position of the N1 acetyl with flexible substituents, the binding energy of the substrate into active site was decreased, which should increase activity against hMAO-A. As classic pharmacophores, heterocyclic rings (piperidine, morpholine, et al.) were also considered to incorporate into the design of the title compound. Herein, based on above rational analysis, we designed and synthesized a series of novel 2-pyrazoline-1-ethanone derivatives used as reversible and selective MAO inhibitors.

2. Results and discussion

2.1. Chemistry

2-Pyrazoline derivatives were synthesized according to the protocol outlined in Schemes 1 and 2. Styrene ketones **1** and **8** were prepared through Claisen–Schmidt condensation of substituted salicylaldehyde with acetophenone and acetone respectively. Compounds **2** and **9** were synthesized by the reaction of excess hydrazine hydrate with **1** and **8**, respectively. The key intermediate compounds **3** and **10** were obtained through the acylation of compounds **2** and **9** with bromoacetyl chloride, respectively. The title compounds **4**–**7** and **11**–**12** were synthesized by the reaction of **3** and **10** with respective azacycle in solvent of acetone.[19,20]

2.2. Crystal structure analysis

The structure of compounds **4f**, **12c** and **12f** were determined by X-ray crystallography. Crystal data of **4f**: colorless crystals, yield, 87%; mp 168–169 °C; $C_{23}H_{26}ClN_3O_3$, M = 427.92, Monoclinic, space group $P2_1/c$; a = 12.1986(4), b = 15.4685(5), c = 12.2638(5) (Å); α = 90, β = 98.683(4), γ = 90, V = 2287.57 (14) Å^3, T = 293(2) K, Z = 4, D_c = 1.242 g/cm^3, $F(000)$ = 904, reflections collected/independent reflections = 4773/4493, data/restraints/parameters = 4493/0/273, Goodness of fit on F^2 = 1.090, fine, R_1 = 0.0522, $wR(F^2)$ = 0.1612. Compound **12c**: colorless crystals, yield, 87%; mp 168–169 °C; $2C_{16}H_{20}N_4O_2Br_2{\cdot}C_2H_5OH$, M = 1012.50, Triclinic, space group $P-1$; a = 9.7322(9), b = 13.7969(14), c = 16.5522(15) (Å); α = 76.557(8), β = 83.763(8), γ = 85.608(8), V = 2145.8(4) Å^3, T = 293(2) K, Z = 2, Dc = 1.567 g/cm^3, $F(000)$ = 1024.0, reflections collected/independent reflections = 15301/8435, data/restraints/parameters = 8435/52/537, Goodness of fit on F^2 = 1.024, Fine, R_1 = 0.0749, $wR(F^2)$ = 0.1799. Compound **12f**: colorless crystals, yield, 70%; mp 177–178 °C; $C_{18}H_{23}N_3O_3Br_2$, M = 489.21, Triclinic, space group $P-1$; a = 7.5225(9), b = 10.4570(20), c = 12.8167(17) (Å); α = 91.154(13), β = 91.637 (11), γ = 99.454(13), V = 993.8(3) Å^3, T = 293(2) K, Z = 2, Dc = 1.635 g/cm^3, $F(000)$ = 492.0, reflections collected/independent reflections = 6601/3897, data/restraints/parameters = 3897/0/238, Goodness of fit on F^2 = 1.040, Fine, R_1 = 0.0518, $wR(F^2)$ = 0.1202.

The molecular structures of compounds **4f**, **12c** and **12f** were shown in Figure 1. Crystallographic data (excluding structure factors) for the structure had been deposited with the Cambridge Crystallographic Data Center as supplementary publication No. CCDC 1021033, 976177, 976176.[21]

2.3. Inhibition of hMAO

The potential effects of the synthesized compounds on hMAO activity were investigated by measuring their effects on the production of hydrogen peroxide (H_2O_2) from *p*-tyramine, using the Amplex Red MAO assay kit (Molecular Probes, Inc., Eugene, Oregon, USA) and MAO isoforms in microsomes prepared from insect cells infected with Recombinant baculovirus containing cDNA inserts for hMAO-A or hMAO-B. The inhibition of hMAO activity was evaluated using the general method described by Santana.[22] The test compounds did not show any interference with the reagents used for a biochemical assay. The results of hMAO-A and hMAO-B inhibition studies with title compounds were reported in Table 1 together with the MAO-A selectivity index.

Enzymatic assays revealed that most of tested compounds exhibited strong inhibitory activity against hMAO, showing

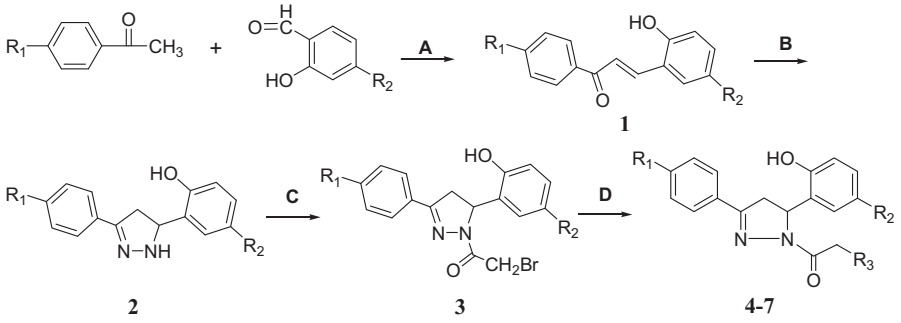

R_2			H					Cl			
R_1			CH_3O	CH_3	H	F	Cl	CH_3O	CH_3	F	Cl
R_3	4	N	**4a**	**4b**	**4c**	**4d**	**4e**	**4f**	**4g**	**4h**	**4i**
	5	N O	**5a**	**5b**	**5c**	**5d**	**5e**	**5f**	**5g**	**5h**	**5i**
	6	N N	**6a**	**6b**	**6c**	**6d**		**6f**	**6g**	**6h**	

3c: R_1 = F, R_2 = H, R_3 = Br **3g:** R_1 = CH_3, R_2 = Cl, R_3 = Br **7h:** R_1 = F, R_2 = Cl, R_3 = N NH

Scheme 1. Synthesis of title compounds **3**∼**7**. Reagents and conditions: (A) NaOH solution, ethanol, 60 °C, 4∼10 h; (B) $N_2H_4{\cdot}H_2O$, ethanol, reflux, 3∼6 h; (C) 2-bromoacetyl chloride, DMAP, CH_2Cl_2, rt, overnight; (D) amine, DMF, KI, NEt_3, 40 °C, 6 h.

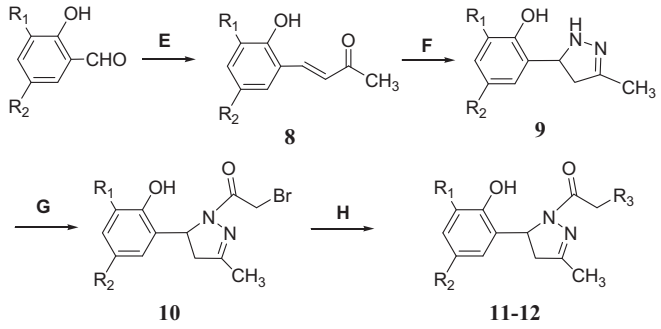

	11a	11b	11c	12a	12b	12c	12d	12e	12f
R_1	H	H	H	Br	Br	Br	Br	Br	Br
R_2	Cl	Cl	Cl	Br	Br	Br	Br	Br	Br
R_3	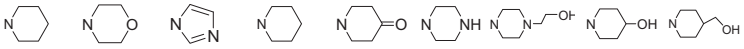								

Scheme 2. Synthesis of title compounds **11**∼**12**. Reagents and conditions: (E) CH_3COCH_3, NaOH solution, 40 °C, 4∼10 h; (F) $N_2H_4{\cdot}H_2O$, ethanol, reflux, 3∼6 h; (G) 2-bromoacetyl chloride, DMAP, CH_2Cl_2, rt, overnight; (H) amine, acetone, KI, NEt_3, 40 °C, 6 h.

selectivity toward hMAO-A. It is obvious from the data that compounds **7h** and **12c** exhibited high activity against hMAO-A with IC_{50} values of 2.40 and 2.00 μM, respectively, surpassing that of the positive control Clorgyline (2.76 μM).[14] Among them, compound **12c** (IC_{50} = 2.00 μM) showed the best activity and higher selectivity (30.0-fold vs 1-fold) with respect to the hMAO-A isoform. Inspection of the chemical structures, it can be concluded that among all synthetic compounds, two classifications can be made, one series is 3,5-diaryl-2-pyrazolines which include compounds **3**∼**7** (Scheme 1), and the other series is 5-aryl-3-methyl-2-pyrazolines which include compounds **11** and **12** (Scheme 2). Both series showed similar inhibitory activity against hMAO-A, such as, IC_{50} values ranging from 2.00 μM to 12.80 μM for active compounds with bromo, piperidinyl or piperazidinyl substituent in the ethanone at N1 position. The results suggested that the substituent at C3 position in the pyrazoline nucleus with the N1 acetyl has little effect on MAO-A inhibitory activity, but, the lack of substituent at C5 led to a lower MAO-A inhibitory activity.[9,23] This pointed out the direction for us to further optimize the structures of 3-methyl-2-pyrazoline derivatives as selective and potential hMAO-A inhibitors.

The importance of the N1 substituent for MAO-A inhibition was demonstrated by the finding that the substituent at N1 ethanone position affected MAO-A inhibitory activity (Table 1). The order of activity of N1 ethanone substituent was bromo (**3**) > piperidinyl (**4**) > morpholinyl (**5**) > imidazolyl (**6**). Amongst compounds with rigid imidazolyl substituent showed inactive (>60 μM) besides **6d** and **11c** (IC_{50} = 26.28 and 30.30 μM) for hMAO-A, instead, compound **6g** showed inhibitory activity and selectivity against MAO-B (IC_{50} = 16.09 μM, SI MAO-A = 0.27). Moreover, compounds with piperazidinyl substituent exhibited highest MAO-A inhibition potency recorded for **7h** (IC_{50} = 2.40 μM) and **12c** (IC_{50} = 2.00 μM). These results showed that the N1 ethanone substituent was critical for the hMAO-A inhibitory activity of 2-pyrazoline system, amongst, bromo, piperazidinyl or piperidinyl substituent at N1 ethanone was found better in terms of potency than the other.

Scanning from the Table 1, the activity of title compounds with piperidinyl groups at N1 ethanone position (compounds **4a**∼**4i**), 5-chloro substitution (compounds **4f**∼**4i**) in the aryl ring at C5 position was found better in terms of potency than unsubstituent (compounds **4a**∼**4e**). The order of activity for *para*-substituent in the aryl ring at C3 position (compounds **4a**–**4e**) is Cl (**4e**) > F (**4d**) > H (**4c**) > CH_3 (**4b**) > CH_3O (**4a**). Similarly, for compounds (**4f**∼**4i**) the order of activity is F (**4h**) > Cl (**4i**) > CH_3O (**4f**) > CH_3 (**4g**). Compounds with electron-withdrawing substituents (fluoro, chloro) at C3 or C5 phenyl ring of the pyrazoline nucleus showed stronger inhibitory activity towards MAO-A.

2.4. Molecular docking

In order to gain more details on the SAR of the title compound which exhibited strong inhibitory activity against hMAO-A, molecular docking of the most potent compounds **7h** and **12c** with hMAO-A was performed on the binding model based on the hMAO-A complex structure (PDB code 2BXR) using the Discovery Studio 3.1 software.[9,24] The binding energy of of compounds **7h** and **12c** was listed in Table 2. Of the compounds studied, compound **7h** was nicely bound into the active site of MAO-A with minimum binding energy ΔG_b = −59.4061 kcal/mol while ΔG_b value of compound **12c** was −59.0684 kcal/mol. Both had nice binding affinity to hMAO-A and their -EDOCKER_INTERACTION_ENERGY had the same trend as the inhibitory activities, which proved the correlation between the inhibitory activity and the binding affinity.

In the result of molecular docking, compounds **7h** and **12c** had almost equal -EDOCKER_INTERACTION_ENERGY, which suggested that both were mostly easy to bind into hMAO-A. The binding model of compounds **7h** and **12c** with hMAO-A complex was respectively depicted in Figures 2 and 3. The 2D and 3D pictures of binding were depicted in figures A and B. Of the 20 residues constituting the active site,[2] more than half anchored the high active compound (**7h** or **12c**), which revealed that title molecule was well filled into the active pocket to display high inhibitory activity. Compound **7h** was nicely bound to hMAO-A via two hydrogen bonds with SER209 (distance = 2.07 Å) and GLU216 (distance = 2.15 Å), and one Pi–Pi interaction between C5 phenyl ring of the pyrazoline and TYR444. Meanwhile, compound **12c** was nicely bound to hMAO-A via three hydrogen bonds with SER209 (distance = 2.06 Å), GLU216 (distance = 2.45 Å) and TYR69 (distance = 1.99 Å), and one Sigma–Pi interaction between C5 phenyl ring of 2-pyrazoline and LYS305. This further supported that compound **12c** with more interactions showed higher inhibitory activity.

Furthermore, when the piperazine-ring of compounds **7h** and **12c** anchored two same residues (SER209 and GLU216) via

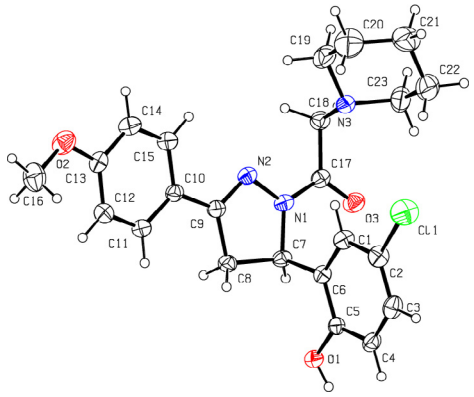

Compound **4f**

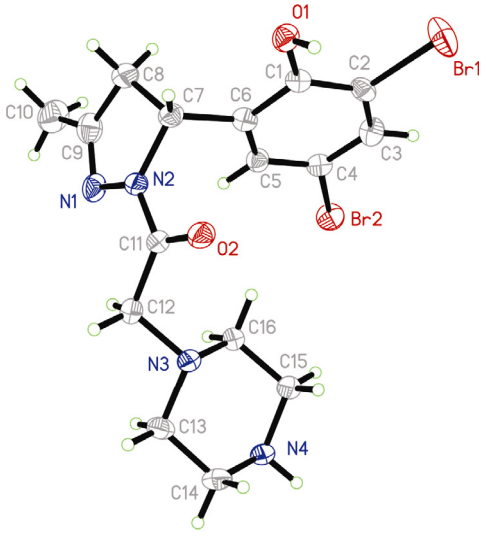

Compound **12c**

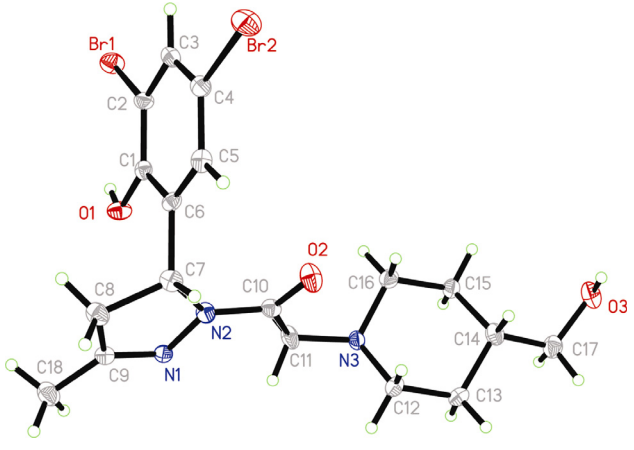

Compound **12f**

Figure 1. ORTEP drawing of compounds **4f**, **12c** and **12f**.

Table 1
IC_{50} values and hMAO-A selectivity index for the new compounds[a]

Compound	MAO-A (μM)	MAO-B (μM)	SI MAO-A[c]
3c	6.00 ± 0.25	52.88 ± 2.01	8.8
3g	5.22 ± 0.20	b	11.5[d]
4a	12.71 ± 0.89	59.40 ± 1.48	4.7
4b	11.32 ± 0.77	45.61 ± 1.60	4.0[d]
4c	9.51 ± 0.79	50.58 ± 2.10	5.3
4d	8.02 ± 0.50	47.36 ± 1.64	5.9
4e	7.25 ± 0.61	40.09 ± 1.97	5.5
4f	9.65 ± 1.01	b	6.2[d]
4g	14.40 ± 1.11	56.21 ± 1.69	3.9
4h	3.72 ± 0.23	b	16.1[d]
4i	6.01 ± 0.40	44.09 ± 0.79	7.3
5a	24.52 ± 1.65	b	2.5[d]
5b	20.01 ± 1.93	b	3.0[d]
5c	23.16 ± 1.50	b	2.6[d]
5d	16.86 ± 1.49	b	3.6[d]
5e	21.20 ± 0.99	31.55 ± 2.04	1.5
5f	18.33 ± 1.26	56.50 ± 2.85	3.1
5g	27.01 ± 1.09	b	2.2[d]
5h	24.30 ± 1.41	30.17 ± 1.29	1.2
5i	31.24 ± 1.72	55.10 ± 2.04	1.8
6a	b	b	
6b	b	41.32 ± 2.00	0.69[d]
6c	b	59.40 ± 2.87	1.0[d]
6d	26.28 ± 1.77	b	2.3[d]
6f	b	b	
6g	b	16.09 ± 1.55	0.27[d]
6h	b	b	
7h	2.40 ± 0.14	58.91 ± 1.80	24.5
11a	10.47 ± 0.36	55.85 ± 2.11	5.3
11b	13.08 ± 0.44	41.80 ± 2.50	3.2
11c	30.30 ± 0.69	b	2.0[d]
12a	7.80 ± 0.60	49.89 ± 2.12	6.4
12b	8.38 ± 0.29	58.94 ± 2.35	7.0
12c	2.00 ± 0.11	b	30.0[d]
12d	12.29 ± 0.41	42.32 ± 1.20	3.4
12e	12.44 ± 0.75	b	4.8[d]
12f	25.65 ± 1.77	30.08 ± 1.36	1.2
Clorgyline	2.76 ± 0.10	b	
Selegiline	b	2.82 ± 0.07	

[a] Each IC_{50} value is the mean ± SEM from three experiments ($n = 3$).
[b] Inactive at 60 μM (highest concentration tested).
[c] SI MAO-A = [IC_{50}(MAO-B)]/[IC_{50}(MAO-A)].
[d] Values obtained under the assumption that the corresponding IC_{50} against either MAO-A or MAO-B is the highest concentration tested (60 μM).

Table 2
EDOCKER_INTERACTION_ENERGY of title compounds and 2BXR

Compound	-EDOCKER_INTERACTION_ENERG ΔG (kcal/mol)	MAO-A (μM)
7h	−59.4061	2.40 ± 0.14
12c	−59.0684	2.00 ± 0.11

hydrogen bonds, smaller steric hindrance at C3 position (–CH_3) led compound **12c** to be better bound into the active pocket (one more hydrogen bond). Moreover, hydrophobic part of two compounds was observed to enter into the 'aromatic cage' involving two nearly parallel tyrosyl residues (407 and 444) to inhibit amine oxidation. These molecular docking results, along with the biological assay data, suggested that compound **12c** possesses higher inhibitory activity than compound **7h**, which will help us carry out structure optimization for rational drug design.

3. Conclusions

In summary, we synthesized a series of novel 2-pyrazoline-1-ethanone derivatives as selective and efficient MAO-A inhibitors, followed by chemical synthesis and biological evaluated for them.

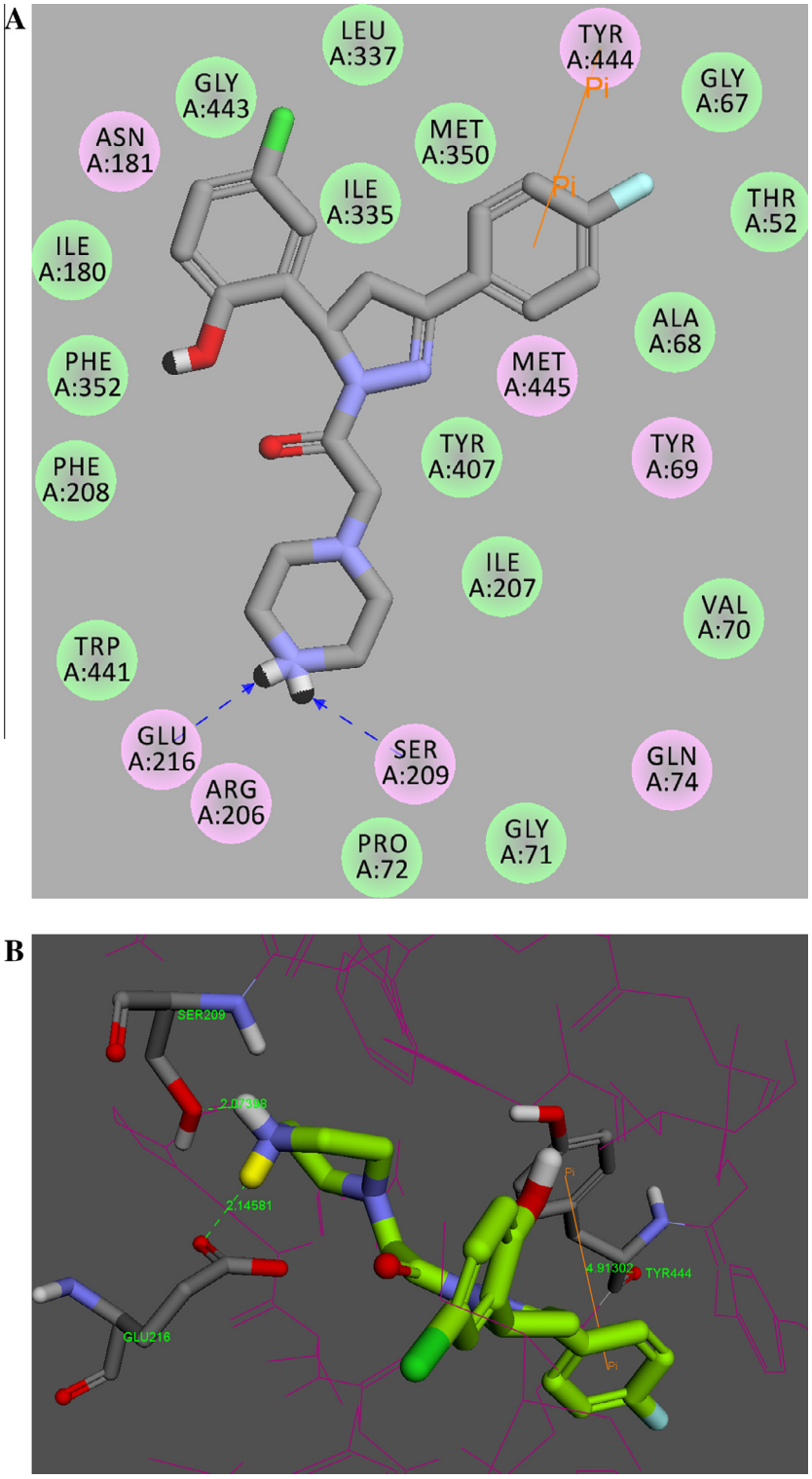

Figure 2. Molecular docking modeling of compound **7h**. (A) 2D Ligand interaction diagram of compound **7h** with MAO-A using Discovery Studio program with the essential amino acid residues at the binding site are tagged in circles. The purple circles show animo acids which related to hydrogen bonding, electrostatic or polar interactions and the green circles show the animo acids related to Van der Waals interactions. (B) Compound **7h** is bond into MAO-A (entry 2BXR.pdb). The dotted lines show the hydrogen bond interaction.

Among them, compounds with piperazidinyl group **7h** (IC_{50} = 2.40 μM) and **12c** (IC_{50} = 2.00 μM) exhibited best inhibitory activity against hMAO-A and higher hMAO-A selectivity than the others, surpassing that of the positive control Clorgyline (IC_{50} = 2.76 μM). SAR analysis showed that the order of N1 substituent affecting hMAO-A inhibitory activity was bromo (**3**) > piperidinyl (**4**) > morpholinyl (**5**) > imidazolyl (**6**), and compounds with electron-withdrawing substituents (-F, -Cl) at C3 or C5 phenyl ring of 2-pyrazoline nucleus had a stronger inhibitory activity towards MAO-A. In addition, the substituent at C3 position

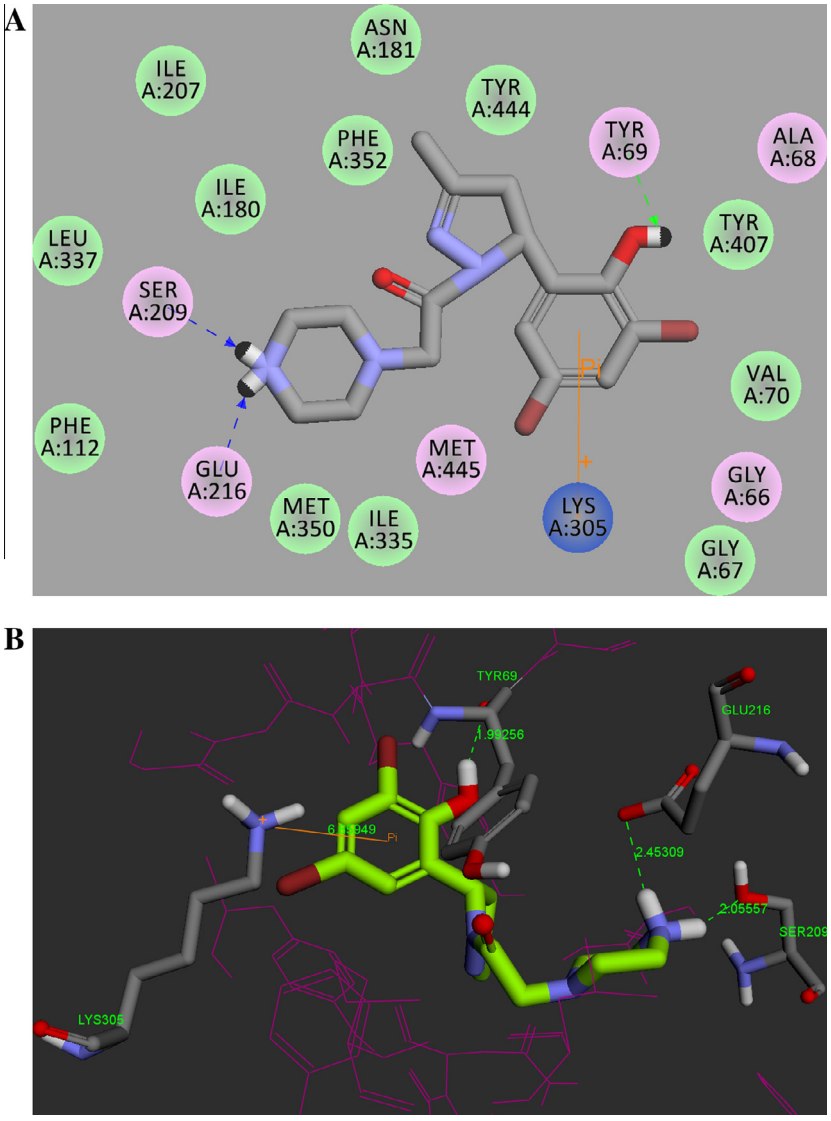

Figure 3. Molecular docking modeling of compound **12c**. (A) 2D Ligand interaction diagram of compound **12c** with MAO-A using Discovery Studio program with the essential amino acid residues at the binding site are tagged in circles. The purple circles show animo acids which related to hydrogen bonding, electrostatic or polar interactions and the green circles show the animo acids related to Van der Waals interactions. (B) Compound **12c** is bond into MAO-A (entry 2BXR.pdb). The dotted lines show the hydrogen bond interaction.

of 2-pyrazoline with the N1 acetyl has little effect on MAO-A inhibitory activity. Furthermore, molecular docking showed that compounds **7h** and **12c** with almost equal binding energy were nicely bound to hMAO-A via two hydrogen bonds (SER209, GLU216) and one Pi–Pi interaction, and three hydrogen bonds (SER209, GLU216, TYR69) and one Sigma–Pi interaction, respectively. Therefore, this novel 3-methyl-2-pyrazoline-1-ethanone moiety might be provided some motivations in the design process as selective and potential hMAO-A inhibitors in the future.

4. Experimental section

4.1. Chemistry

The reactions were monitored by thin layer chromatography (TLC) on pre-coated silica GF_{254} plates. Melting points (uncorrected) were determined on a XT4MP apparatus (Taike Corp., Beijing, China). ^{1}H and ^{13}C NMR spectra were collected on Bruker AV300 spectrometer at room temperature with TMS and solvent signals allotted as internal standards. Chemical shifts are reported in ppm (δ). Mass spectra were performed on an Agilent 1260–6221 TOF mass spectrometer. IR spectra were recorded on a Shimadzu IRPrestige-21 spectrophotometer.

4.2. General procedure for the synthesis of title compounds 3–7

To a solution of aromatic methyl ketones (10 mmol) and salicylaldehyde (11 mmol) in ethanol (10 mL) was added 40% NaOH aqueous solution (2 mL) dropwise and the reaction was carried out at 60 °C for 4∼10 h until the disappearance of starting material (monitored by thin layer chromatography). The mixture was poured into cold water and neutralized with 2 M HCl to a pH in the range of 2∼3. The resulting precipitate was collected, washed with water and dried to give chalcones (**1**). The chalcone (**1**) was treated with 5 times excess of hydrazine hydrate in dry ethanol and refluxed for 3∼6 h. The reaction mixture was then poured into ice-cold water. The solid was filtered, washed and recrystallized from ethanol to afford respective pyrazoline (**2**). A mixture of compound **2** and bromoacetyl chloride in CH_2Cl_2 was added

4-dimethylaminopyridine (DMAP) and the reaction was carried out overnight. The reaction mixture was washed with H_2O and brine. The resulting residue was then purified by column chromatography to give the N-acylated product **3**. A catalytic amount of KI was added to a DMF (20 mL) solution of compound **3** (2.0 mmol), the amine (3.0 mmol) and triethylamine (0.40 mL), then the reaction mixture were stirred at 40 °C for 6 h. The mixture was allowed to cool to room temperature and 30 mL water was added, allowed to stand at 0 °C overnight. The product was collected by filtration and the residue was purified by chromatography on a silica gel column (petroleum/EtOAc, 1:1 → 1:3) to give title compounds **4**∼**7**.

4.2.1. Compound 3c

2-Bromo-1-(5-(2-hydroxy-phenyl)-3-(4-fluoro-phenyl)-4,5-dihydro-pyrazol-1-yl)-ethanone, white powder, yield, 40%; mp 178–180 °C; IR (KBr, ν/cm^{-1}): 3256 (ν_{O-H}), 2929 (ν_{asC-H}), 2857 (ν_{sC-H}), 1639 ($\nu_{C=O}$), 1600 ($\nu_{ArC=C}$), 1471 ($\nu_{ArC=C}$), 838 ($\gamma_{=C-H}$), 754 ($\gamma_{=C-H}$); ^{1}H (300 MHz, DMSO-d_6) δ (ppm): 3.08 (dd, 1H, J_1 = 4.6 Hz, J_2 = 18.0 Hz, 4-Ha), 3.85 (dd, 1H, J_1 = 11.7 Hz, J_2 = 18.0 Hz, 4-Hb), 4.41 (d, 1H, J = 11.0 Hz, Ha), 4.52 (d, 1H, J = 11.0 Hz, Hb), 5.65 (dd, 1H, J_1 = 4.5 Hz, J_2 = 11.7 Hz, 5-H), 6.77–7.91 (8H, Ar-H), 9.73 (s, 1H). TOF-HRMS: m/z [M+H]$^+$ calcd for $C_{17}H_{15}BrFN_2O_2$: 377.0295; found: 377.0297.

4.2.2. Compound 3g

2-Bromo-1-(5-(5-chloro-2-hydroxy-phenyl)-3-(4-methyl-phenyl)-4,5-dihydro-pyrazol-1-yl)-ethanone, white powder, yield, 38%; mp 185–187 °C; IR (KBr, ν/cm^{-1}): 3267 (ν_{O-H}), 2921 (ν_{asCH2}), 1639 ($\nu_{C=O}$), 1599 ($\nu_{ArC=C}$), 1469 ($\nu_{ArC=C}$), 815 ($\gamma_{=C-H}$); ^{1}H (300 MHz, DMSO-d_6) δ (ppm): 2.35 (s, 3H, CH_3), 3.08 (dd, 1H, J_1 = 4.7 Hz, J_2 = 18.0 Hz, 4-Ha), 3.83 (dd, 1H, J_1 = 11.7 Hz, J_2 = 18.0 Hz, 4-Hb), 4.38 (d, 1H, J = 11.0 Hz, Ha), 4.55 (d, 1H, J = 11.0 Hz, Hb), 5.60 (dd, 1H, J_1 = 4.6, J_2 = 11.7 Hz, 5-H), 6.76–7.76 (7H, Ar-H), 10.09 (s, 1H). TOF-HRMS: m/z [M+H]$^+$ calcd for $C_{18}H_{17}BrClN_2O_2$: 407.0156; found: 407.0160.

4.2.3. Compound 4a

1-(5-(2-Hydroxy-phenyl)-3-(4-methoxy-phenyl)-4,5-dihydro-pyrazol-1-yl)ethanone-2-piperidine, yellow powder, yield, 18%; mp 168–169 °C; IR (KBr, ν/cm^{-1}): 3418 (ν_{O-H}), 2934 (ν_{asC-H}), 1646 ($\nu_{C=O}$), 1609 ($\nu_{ArC=C}$), 1254 (ν $_{C-O}$), 1043 (ν_{C-O-C}), 833 ($\gamma_{=C-H}$); ^{1}H (300 MHz, DMSO-d_6) δ (ppm): 1.30–1.48 (m, 6H), 2.48–2.58 (m, 4H, overlap, DMSO-d_6, 2× CH_2), 2.94 (dd, 1H, J_1 = 4.4 Hz, J_2 = 17.8 Hz, 4-Ha), 3.51 (d, 1H, J = 15.6 Hz, Ha), 3.66 (d, 1H, J = 15.2 Hz, Hb), 3.74 (dd, 1H, J_1 = 11.5 Hz, J_2 = 17.8 Hz, 4-Hb), 3.79 (s, 3H, CH_3O), 5.62 (dd, 1H, J_1 = 4.3 Hz, J_2 = 11.2 Hz, 5-H), 6.65–7.75 (8H, Ar-H), 9.67 (s, 1H); ^{13}C NMR (75 MHz, DMSO-d_6) δ (ppm): 23.7 (CH_2), 25.5 (2C), 40.7 (4-C), 53.9 (2C), 55.2 (5-C), 55.3 (CH_3O), 59.3, 114.4 (2C), 115.3, 118.7, 123.7, 125.4, 127.7, 128.0, 128.2 (2C), 153.9, 154.4 (3-C), 160.8, 166.5. TOF-HRMS: m/z [M+H]$^+$ calcd for $C_{23}H_{28}N_3O_3$: 394.2125; found: 394.2124.

4.2.4. Compound 4b

1-(5-(2-Hydroxy-phenyl)-3-(4-methyl-phenyl)-4,5-dihydro-pyrazol-1-yl)ethanone-2-piperidine, white powder, yield, 15%; mp 166–167 °C; ^{1}H (300 MHz, $CDCl_3$) δ (ppm): 1.35–1.69 (m, 6H), 2.43 (s, 3H, CH_3), 2.50–2.62 (m, 4H), 3.48 (dd, 1H, J_1 = 3.5 Hz, J_2 = 17.9 Hz, 4-Ha), 3.64 (d, 2H, J = 6.8 Hz, Ha, Hb), 3.70 (dd, 1H, J_1 = 3.5 Hz, J_2 = 17.9 Hz, 4-Hb), 5.81 (dd, 1H, J_1 = 3.5 Hz, J_2 = 11.2 Hz, 5-H), 6.79–7.75 (8H, Ar-H), ^{13}C NMR (75 MHz, $CDCl_3$) δ (ppm): 21.6 (CH_3), 24.0 (CH_2), 25.8 (2C), 39.7 (4-C), 53.9 (5-C), 54.9 (2C), 59.7, 119.0, 120.8, 125.9, 126.9 (2C), 127.4, 128.1, 129.6 (2C), 129.7, 141.4, 155.1, 156.9 (3-C), 168.8. TOF-HRMS: m/z [M+H]$^+$ calcd for $C_{23}H_{28}N_3O_2$: 378.2176; found: 378.2176.

4.2.5. Compound 4c

1-(5-(2-Hydroxy-phenyl)-3-(phenyl)-4,5-dihydro-pyrazol-1-yl) ethanone-2-piperidine, white powder, yield, 17%; mp 197–199 °C; IR (KBr, ν/cm^{-1}): 3423 (ν_{O-H}), 2919 (ν_{asC-H}), 1663 ($\nu_{C=O}$), 1595 ($\nu_{ArC=C}$), 1453 ($\nu_{ArC=C}$), 867 ($\gamma_{=C-H}$), 752 ($\gamma_{=C-H}$); ^{1}H (300 MHz, DMSO-d_6) δ (ppm): 1.31–1.88 (m, 6H), 2.93–3.60 (m, 5H, 4-Ha), 3.89 (dd, 1H, J_1 = 11.7 Hz, J_2 = 18.1 Hz, pyrazole 4-Hb), 4.53 (d, 1H, J = 17.1 Hz, Ha), 4.65 (d, 1H, J = 17.0 Hz, Hb), 5.70 (dd, 1H, J_1 = 4.8 Hz, J_2 = 11.6 Hz, 5-H), 6.69–7.88 (9H, Ar-H), 9.55 (s, 1H); ^{13}C NMR (75 MHz, DMSO-d_6) δ (ppm): 21.2 (CH_2), 22.3 (2C), 40.8 (4-C), 53.3 (2C), 56.4 (C-5), 56.6, 115.5, 118.8, 126.4, 126.6, 127.0 (2C), 128.5, 128.8 (2C), 130.5, 130.9, 154.2, 157.5 (3-C), 161.5. TOF-HRMS: m/z [M+H]$^+$ calcd for $C_{22}H_{26}N_3O_2$: 364.2020; found: 364.2017.

4.2.6. Compound 4d

1-(5-(2-Hydroxy-phenyl)-3-(4-fluoro-phenyl)-4,5-dihydro-pyrazol-1-yl)ethanone-2-piperidine, yellow powder, yield, 14%; mp 183–185 °C; ^{1}H (300 MHz, DMSO-d_6) δ (ppm): 1.23–1.59 (m, 6H), 2.48–2.58 (m, 4H, overlap, DMSO-d_6, 2× CH_2), 2.98 (dd, 1H, J_1 = 4.5 Hz, J_2 = 17.9 Hz, 4-Ha), 3.51 (d, 1H, J = 15.7 Hz, Ha), 3.67 (d, 1H, J = 15.7 Hz, Hb), 3.77 (dd, 1H, J_1 = 11.8 Hz, J_2 = 17.9 Hz, 4-Hb), 5.64 (dd, 1H, J_1 = 4.5 Hz, J_2 = 11.8 Hz, 5-H), 6.60–7.89 (8H, Ar-H), 9.67 (s, 1H); ^{13}C NMR (75 MHz, DMSO-d_6) δ (ppm): 23.7 (CH_2), 25.6 (2C), 40.6 (4-C), 53.9 (2C), 55.6 (5-C), 59.3, 115.3, 115.6, 115.9, 118.7, 125.6, 127.6, 127.9 (2C), 128.0, 128.8, 128.9, 153.7 (3-C), 153.9, 166.8. TOF-HRMS: m/z [M+H]$^+$ calcd for $C_{22}H_{25}FN_3O_2$: 382.1925; found: 382.1928.

4.2.7. Compound 4e

1-(5-(2-Hydroxy-phenyl)-3-(4-chloro-phenyl)-4,5-dihydro-pyrazol-1-yl)ethanone-2-piperidine, white powder, yield, 14%; mp 210–212 °C; IR (KBr, ν/cm^{-1}): 3305 (ν_{O-H}), 2847 (ν_{sC-H}), 1636 ($\nu_{C=O}$), 1461 ($\nu_{ArC=C}$), 1229 (ν_{C-O}), 1117, 840 ($\gamma_{=C-H}$), 760 ($\gamma_{=C-H}$); ^{1}H (300 MHz, DMSO-d_6) δ (ppm): 1.29–1.55 (m, 6H), 2.48–2.58 (m, 4H, overlap, DMSO-d_6, 2× CH_2), 2.98 (dd, 1H, J_1 = 4.6 Hz, J_2 = 17.9 Hz, 4-Ha), 3.41–3.89 (m, 3H, 4-Hb, Ha, Hb), 5.64 (dd, 1H, J_1 = 4.5 Hz, J_2 = 11.8 Hz, 5-H), 6.63–7.84 (8H, Ar-H), 9.68 (s, 1H); ^{13}C NMR (75 MHz, DMSO-d_6) δ (ppm): 23.7 (CH_2), 25.6 (2C), 40.4 (4-C), 53.9 (2C), 55.7 (5-C), 59.3, 115.4, 118.7, 125.7, 127.5, 128.1, 128.3 (2C), 128.8 (2C), 130.2, 134.7, 153.6 (3-C), 153.9, 166.9. TOF-HRMS: m/z [M+H]$^+$ calcd for $C_{22}H_{25}ClN_3O_2$: 398.1630; found: 398.1631.

4.2.8. Compound 4f

1-(5-(5-Chloro-2-hydroxy-phenyl)-3-(4-methoxy-phenyl)-4,5-dihydro-pyrazol-1-yl)ethanone-2-piperidine, yellow crystals, yield, 18%; mp 180–182 °C; ^{1}H (300 MHz, DMSO-d_6) δ (ppm): 1.26–1.59 (m, 6H), 2.48–2.58 (m, 4H, overlap, DMSO-d_6, 2× CH_2), 2.98 (dd, 1H, J_1 = 4.6 Hz, J_2 = 17.9 Hz, 4-Ha), 3.42 (d, 1H, J = 15.7 Hz, Ha), 3.67–3.84 (m, 5H, Hb, CH_3O, 4-Hb), 5.58 (dd, 1H, J_1 = 4.6 Hz, J_2 = 11.7 Hz, 5-H), 6.75–7.76 (7H, Ar-H), 10.04 (s, 1H); ^{13}C NMR (75 MHz, DMSO-d_6) δ (ppm): 23.8 (CH_2), 25.7 (2C), 40.4 (4-C), 54.0 (2C), 55.0 (5-C), 55.3 (CH_3O), 59.4, 114.2 (2C), 117.0, 122.4, 123.6, 125.3, 127.7, 128.3 (2C), 129.8, 153.0, 154.5 (3-C), 160.9, 166.8. TOF-HRMS: m/z [M+H]$^+$ calcd for $C_{23}H_{27}ClN_3O_3$: 428.1735; found: 428.1738.

4.2.9. Compound 4g

1-(5-(5-Chloro-2-hydroxy-phenyl)-3-(4-methyl-phenyl)-4,5-dihydro-pyrazol-1-yl)ethanone-2-piperidine, yellow powder, yield, 16%; mp 153–155 °C; ^{1}H (300 MHz, DMSO-d_6) δ (ppm): 1.25–1.60 (m, 6H), 2.31 (s, 3H, CH_3), 2.48–2.58 (m, 4H, overlap, DMSO-d_6, 2× CH_2), 2.99 (dd, 1H, J_1 = 4.7 Hz, J_2 = 17.9 Hz, 4-Ha), 4.38 (d, 1H, J = 15.5 Hz, Ha), 3.66–3.85 (m, 2H, 4-Hb, Hb), 5.58 (dd, 1H, J_1 = 4.7, J_2 = 11.8 Hz, 5-H), 6.72–7.76 (7H, Ar-H), 10.04 (s,

1H); ^{13}C NMR (75 MHz, DMSO-d_6) δ (ppm): 21.0 (CH_3), 23.7 (CH_2), 25.6 (2C), 40.3 (4-C), 54.0 (2C), 55.1 (5-C), 59.3, 117.0, 122.3, 125.3, 126.6 (2C), 127.7, 128.3, 129.3 (2C), 129.7, 140.1, 153.0, 154.7 (3-C), 166.8. TOF-HRMS: m/z $[M+H]^+$ calcd for $C_{23}H_{27}ClN_3O_2$: 412.1786; found: 412.1789.

4.2.10. Compound 4h

1-(5-(5-Chloro-2-hydroxy-phenyl)-3-(4-fluoro-phenyl)-4,5-dihydro-pyrazol-1-yl)ethanone-2-piperidine, yellow crystals, yield, 16%; mp 186–187 °C; ^{1}H (300 MHz, DMSO-d_6) δ (ppm): 1.24–1.62 (m, 6H), 2.48–2.58 (m, 4H, overlap, DMSO-d_6, 2× CH_2), 3.03 (dd, 1H, J_1 = 4.8 Hz, J_2 = 18.0 Hz, 4-Ha), 3.42 (d, 1H, J = 15.4 Hz, Ha), 3.89–3.65 (m, 2H, 4-Hb, Hb), 5.60 (dd, 1H, J_1 = 4.8 Hz, J_2 = 11.9 Hz, 5-H), 6.79–7.79 (7H, Ar-H), 10.05 (s, 1H); TOF-HRMS: m/z $[M+H]^+$ calcd for $C_{22}H_{24}ClFN_3O_2$: 416.1536; found: 416.1533.

4.2.11. Compound 4i

1-(5-(5-Chloro-2-hydroxy-phenyl)-3-(4-chloro-phenyl)-4,5-dihydro-pyrazol-1-yl)ethanone-2-piperidine, white powder, yield, 18%; mp 156–158 °C; IR (KBr, ν/cm^{-1}): 3420 (ν_{O-H}), 2931 (ν_{asC-H}), 1658 ($\nu_{C=O}$), 1468 ($\nu_{ArC=C}$), 816 ($\gamma_{=C-H}$); ^{1}H (300 MHz, DMSO-d_6) δ (ppm): 1.37–1.82 (m, 6H), 2.48–2.58 (m, 4H, overlap, DMSO-d_6, 2× CH_2), 3.16 (dd, 1H, J_1 = 5.1 Hz, J_2 = 18.1 Hz, 4-Ha), 3.84 (dd, 1H, J_1 = 11.9 Hz, J_2 = 18.1 Hz, 4-Hb), 4.26 (d, 1H, 1H, J = 17.1 Hz, Ha), 4.41 (d, 1H, J = 17.0 Hz, Hb), 5.64 (dd, 1H, J_1 = 5.1 Hz, J_2 = 11.9 Hz, 5-H), 6.85–7.91 (7H, Ar-H), 10.24 (s, 1H); ^{13}C NMR (75 MHz, DMSO-d_6) δ (ppm): 21.9 (CH_2), 23.2 (2C), 40.3 (4-C), 53.4 (2C), 56.3 (5-C), 57.0, 117.2, 122.1, 126.2, 128.0, 128.5, 128.6 (2C), 128.9 (2C), 129.5, 135.3, 153.4, 155.8 (3-C), 163.3. TOF-HRMS: m/z $[M+H]^+$ calcd for $C_{22}H_{24}Cl_2N_3O_2$: 432.1240; found: 432.1238.

4.2.12. Compound 5a

1-(5-(2-Hydroxy-phenyl)-3-(4-methoxy-phenyl)-4,5-dihydro-pyrazol-1-yl)ethanone-2-morpholine, white powder, yield, 19%; mp 117–118 °C; ^{1}H (300 MHz, $CDCl_3$) δ (ppm): 2.76–2.50 (m, 4H), 3.48 (dd, 1H, J_1 = 3.4 Hz, J_2 = 17.9 Hz, 4-Ha), 3.57–3.71 (m, 3H, Ha, Hb, 4-Hb), 3.71–3.82 (m, 4H), 3.89 (s, 3H, CH_3O), 5.81 (dd, 1H, J_1 = 3.4 Hz, J_2 = 11.2 Hz, 5-H), 6.79–7.83 (8H, Ar-H), 9.10 (s, 1H); ^{13}C NMR (75 MHz, $CDCl_3$) δ (ppm): 39.9 (4-C), 53.9 (2C), 55.5 (5-C, CH_3O), 59.3, 66.8 (2C), 114.3 (2C), 118.9, 120.9, 123.3, 125.8, 127.2, 128.6 (2C), 129.7, 154.9 (3-C), 157.0, 161.9, 168.0. TOF-HRMS: m/z $[M+H]^+$ calcd for $C_{22}H_{26}N_3O_{4:}$ 396.1918; found: 396.1919.

4.2.13. Compound 5b

1-(5-(2-Hydroxy-phenyl)-3-(4-methyl-phenyl)-4,5-dihydro-pyrazol-1-yl)ethanone-2-morpholin yellow powder, yield 17%, mp 177–179 °C; IR (KBr, ν/cm^{-1}): 3421 (ν_{O-H}), 2955 (ν_{asC-H}), 2924 (ν_{asC-H}), 2855 (ν_{sC-H}), 2798 (ν_{sC-H}), 1647 ($\nu_{C=O}$), 1455 ($\nu_{ArC=C}$), 1115 (ν_{C-O-C}); ^{1}H (300 MHz, DMSO-d_6) δ (ppm): 2.34 (s, 3H, CH_3), 2.52–2.64 (m, 4H), 2.96 (dd, 1H, J_1 = 4.5 Hz, J_2 = 17.8 Hz 4-Ha), 3.51–3.62 (m, 5H, Ha), 3.83–3.66 (m, 2H, Hb, 4-Hb), 5.63 (dd, 1H, J_1 = 4.4 Hz, J_2 = 11.7 Hz, 5-H), 6.65–7.56 (8H, Ar-H), 9.67 (s, 1H); ^{13}C NMR (75 MHz, DMSO-d_6) δ (ppm): 21.0 (CH_3), 40.6 (4-C), 53.1 (2C), 55.4 (5-C), 58.8, 66.2 (2C), 115.4, 118.8, 125.5, 126.6 (2C), 127.6, 128.0, 128.4, 129.3 (2C), 140.0, 153.9, 154.9 (3-C), 166.3. TOF-HRMS: m/z $[M+H]^+$ calcd for $C_{22}H_{26}N_3O_3$: 380.1969; found: 380.1971.

4.2.14. Compound 5c

1-(5-(2-Hydroxy-phenyl)-3-(phenyl)-4,5-dihydro-pyrazol-1-yl) ethanone-2-morpholine white powder, yield, 19%; mp 211–212 °C; ^{1}H (300 MHz, $CDCl_3$) δ (ppm): 2.56–2.72 (m, 4H), 3.51 (dd, J_1 = 3.6 Hz, J_2 = 18.1 Hz, 4-Ha), 3.65–3.74 (m, 3H, 4-Hb, Ha, Hb), 3.74–3.80 (m, 4H), 5.84 (dd, 1H, J_1 = 3.6 Hz, J_2 = 11.3 Hz, 5-H), 6.79–7.90 (9H, Ar-H), 8.98 (s, 1H); ^{13}C NMR (75 MHz, $CDCl_3$) δ (ppm): 39.9 (4-C), 53.9 (2C), 54.1 (5-C), 59.4, 66.8 (2C), 118.9, 121.0, 125.9, 127.0 (2C), 127.1, 128.9 (2C), 129.7, 130.7, 131.0, 154.8, 157.1 (3-C), 168.3. TOF-HRMS: m/z $[M+H]^+$ calcd for $C_{21}H_{24}N_3O_3$: 366.1812; found: 366.1814.

4.2.15. Compound 5d

1-(5-(2-Hydroxy-phenyl)-3-(4-fluoro-phenyl)-4,5-dihydro-pyrazol-1-yl)ethanone-2-morpholine, white powder, yield, 15%; mp 187–188 °C; IR (KBr, ν/cm^{-1}): 3303 (ν_{O-H}), 1637 ($\nu_{C=O}$), 1459 ($\nu_{ArC=C}$), 1227 (ν_{C-O}), 1121 (ν_{C-O-C}), 1041 (ν_{C-O-C}), 867 ($\gamma_{=C-H}$), 760 ($\gamma_{=C-H}$); ^{1}H (300 MHz, DMSO-d_6) δ (ppm): 2.51–2.68 (m, 4H), 3.00 (dd, J_1 = 4.6 Hz, J_2 = 17.9 Hz, 4-Ha), 3.51–3.85 (m, 7H, Ha, Hb, 4-Hb), 5.64 (dd, 1H, J_1 = 4.5, J_2 = 11.7 Hz, 5-H), 6.64–7.91 (8H, Ar-H), 9.68 (s, 1H). TOF-HRMS: m/z $[M+H]^+$ calcd for $C_{21}H_{23}FN_3O_3$: 384.1718; found: 384.1719.

4.2.16. Compound 5e

1-(5-(2-Hydroxy-phenyl)-3-(4-chloro-phenyl)-4,5-dihydro-pyrazol-1-yl)ethanone-2-morpholine, yellow powder, yield, 14%; mp 176–177 °C; ^{1}H (300 MHz, DMSO-d_6) δ (ppm): 2.51–2.65 (m, 4H), 3.00 (dd, 1H, J_1 = 4.6 Hz, J_2 = 17.9 Hz, 4-Ha), 3.50–3.83 (m, 7H, Ha, Hb, 4-Hb), 5.64 (dd, 1H, J_1 = 4.5 Hz, J_2 = 11.8 Hz, 5-H), 6.62–7.85 (8H, Ar-H), 9.68 (s, 1H); ^{13}C NMR (75 MHz, DMSO-d_6) δ (ppm): 40.4 (4-C), 53.1 (2C), 55.8 (5-C), 58.8, 66.2 (2C), 115.4, 118.8, 125.7, 127.4, 128.1, 128.3 (2C), 128.8 (2C), 130.1, 134.8, 153.9, 154.0 (3-C), 166.4. TOF-HRMS: m/z $[M+H]^+$ calcd for $C_{21}H_{23}ClN_3O_3$: 400.1422; found: 400.1424.

4.2.17. Compound 5f

1-(5-(5-Chloro-2-hydroxy-phenyl)-3-(4-methoxy-phenyl)-4,5-dihydro-pyrazol-1-yl)ethanone-2-morpholine, white powder, yield, 13%; mp 223–225 °C; ^{1}H (300 MHz, DMSO-d_6) δ (ppm): 2.52–2.65 (m, 4H), 3.00 (dd, 1H, J_1 = 4.6 Hz, J_2 = 17.9 Hz, 4-Ha), 3.47 (d, 1H, J = 15.6 Hz, Ha), 3.58 (t, 4H, J = 4.6 Hz), 3.69–3.84 (m, 5H, Hb, CH_3O, 4-Hb), 5.58 (dd, 1H, J_1 = 4.6 Hz, J_2 = 11.7 Hz, 5-H), 6.67–7.80 (7H, Ar-H), 10.04 (s, 1H). TOF-HRMS: m/z $[M+H]^+$ calcd for $C_{22}H_{25}ClN_3O_4$: 430.1530; found: 430.1530.

4.2.18. Compound 5g

1-(5-(5-Chloro-2-hydroxy-phenyl)-3-(4-methyl-phenyl)-4,5-dihydro-pyrazol-1-yl)ethanone-2-morpholine, white powder, yield, 19%; mp 189–191 °C; IR (KBr, ν/cm^{-1}): 3305 (ν_{O-H}), 2933 (ν_{asC-H}), 2839 (ν_{sC-H}), 1673 ($\nu_{C=O}$), 1607 ($\nu_{ArC=C}$), 1518 ($\nu_{ArC=C}$), 1455 ($\nu_{ArC=C}$), 1251 (ν_{C-O}), 832 ($\gamma_{=C-H}$); ^{1}H (300 MHz, DMSO-d_6) δ (ppm): 2.31 (s, 3H, CH_3), 2.52–2.70 (m, 4H), 3.01 (dd, 1H, J_1 = 4. 7 Hz, J_2 = 17.9 Hz, 4-Ha), 3.48 (d, 1H, J = 15.7 Hz, Ha), 3.58 (t, 4H, J = 4.6 Hz), 3.66–3.86 (m, 2H, 4-Hb, Hb), 5.58 (dd, 1H, J_1 = 4.7 Hz, J_2 = 11.8 Hz, 5-H), 6.68–7.78 (7H, Ar-H), 10.04 (s, 1H). TOF-HRMS: m/z $[M+H]^+$ calcd for $C_{22}H_{25}ClN_3O_3$: 414.1582; found: 414.1582.

4.2.19. Compound 5h

1-(5-(5-Chloro-2-hydroxy-phenyl)-3-(4-fluoro-phenyl)-4,5-dihydro-pyrazol-1-yl)ethanone-2-morpholine, white powder, yield, 16%; mp 199–200 °C; IR (KBr, ν/cm^{-1}): 3410 (ν_{O-H}), 3248 ($\nu_{as=C-H}$), 2859 (ν_{asC-H}), 1649 ($\nu_{C=O}$), 1600 ($\nu_{ArC=C}$), 1466 ($\nu_{ArC=C}$), 1231 (ν_{C-O}), 1112 (ν_{C-O-C}), 839 ($\gamma_{=C-H}$); ^{1}H (300 MHz, DMSO-d_6) δ (ppm): 2.52–2.66 (m, 4H), 3.05 (dd, 1H, J_1 = 4. 8 Hz, J_2 = 18.0 Hz, 4-Ha), 3.49 (d, 1H, J = 15.6 Hz, Ha), 3.58 (t, 4H, J = 4.6 Hz), 3.68–3.87 (m, 2H, 4-Hb, Hb), 5.60 (dd, 1H, J_1 = 4.8 Hz, J_2 = 11.9 Hz, 5-H), 6.77–7.90 (7H, Ar-H), 10.04 (s, 1H); ^{13}C NMR (75 MHz, DMSO-d_6) δ (ppm): 40.3 (4-C), 53.2 (2C), 55.5 (5-C), 58.8, 66.2 (2C), 115.6, 115.9, 117.0, 122.3, 125.5, 127.6, 127.7, 127.8, 129.0, 129.1, 129.5, 153.0, 154.1 (3-C), 166.5. TOF-HRMS: m/z $[M+H]^+$ calcd for $C_{21}H_{22}ClFN_3O_3$: 418.1328; found: 418.1332.

4.2.20. Compound 5i

1-(5-(5-Chloro-2-hydroxy-phenyl)-3-(4-chloro-phenyl)-4,5-dihydro-pyrazol-1-yl)ethanone-2-morpholine, yellow powder, yield, 19%; mp 183–184 °C; ^{1}H (300 MHz, DMSO-d_6) δ (ppm): 2.52–2.65 (m, 4H), 3.05 (dd, 1H, J_1 = 4. 9 Hz, J_2 = 18.0 Hz, 4-Ha), 3.49 (d, 1H, J = 15.7 Hz, Ha), 3.58 (t, 4H, J = 4.6 Hz), 3.70–3.87 (m, 2H, 4-Hb, Hb), 5.60 (dd, 1H, J_1 = 4.9 Hz, J_2 = 11.9 Hz, 5-H), 6.92–7.85 (7H, Ar-H), 10.04 (s, 1H); ^{13}C NMR (75 MHz, DMSO-d_6) δ (ppm): 40.2 (4-C), 53.1 (2C), 55.6 (5-C), 58.7, 66.1 (2C), 117.0, 122.2, 125.5, 127.8, 128.3 (2C), 128.7 (2C), 129.4, 129.9, 134.8, 153.0, 153.9 (3-C), 166.6. TOF-HRMS: m/z [M+H]$^+$ calcd for $C_{21}H_{22}Cl_2N_3O_3$: 434.1033; found: 434.1036.

4.2.21. Compound 6a

1-(5-(2-Hydroxy-phenyl)-3-(4-methoxy-phenyl)-4,5-dihydro-pyrazol-1-yl)ethanone-2-imidazole, yellow powder, yield, 21%; mp 212–213 °C; ^{1}H (300 MHz, DMSO-d_6) δ (ppm): 3.05 (dd, 1H, J_1 = 4.5 Hz, J_2 = 17.8 Hz, 4-Ha), 3.72–3.88 (m, 4H, CH_3O, 4-Hb), 5.28 (d, 1H, J = 17.2 Hz, Ha), 5.42 (d, 1H, J = 17.2 Hz, Hb), 5.63 (dd, 1H, J_1 = 4.4 Hz, J_2 = 11.2 Hz, 5-H), 6.85 (s, 1H, iminazole 5-H), 7.13 (s, 1H, iminazole 4-H), 7.62 (s, 1H, iminazole 2-H), 6.67–7.83 (8H, Ar-H), 9.72 (s, 1H); ^{13}C NMR (75 MHz, DMSO-d_6) δ (ppm): 40.9 (4-C), 47.9 (5-C), 55.3 (CH_3O), 55.9, 114.2 (2C), 115.4, 118.8, 120.9, 123.4, 125.9, 127.1, 127.6, 128.2, 128.5 (2C), 138.4, 154.0 (3-C), 155.9, 161.1, 164.1. TOF-HRMS: m/z [M+H]$^+$ calcd for $C_{21}H_{21}N_4O_3$: 377.1608; found: 377.1607.

4.2.22. Compound 6b

1-(5-(2-Hydroxy-phenyl)-3-(4-methyl-phenyl)-4,5-dihydro-pyrazol-1-yl)ethanone-2-imidazole, yellow powder, yield, 16%; mp 222–224 °C; ^{1}H (300 MHz, DMSO-d_6) δ (ppm): 2.35 (s, 3H, CH_3), 3.06 (dd, 1H, J_1 = 4.6 Hz, J_2 = 17.9 Hz, 4-Ha), 3.82 (dd, 1H, J_1 = 11.7 Hz, J_2 = 18.0 Hz, 4-Hb), 5.29 (d, 1H, J = 17.3 Hz, Ha), 5.45 (d, 1H, J = 17.3 Hz, Hb), 5.64 (dd, 1H, J_1 = 4.5 Hz, J_2 = 11.6 Hz, 5-H), 6.85 (s, 1H, iminazole 5-H), 7.13 (s, 1H, iminazole 4-H), 7.62 (s, 1H, iminazole 2-H), 6.65–7.80 (8H, Ar-H), 9.72 (s, 1H). TOF-HRMS: m/z [M+H]$^+$ calcd for $C_{21}H_{21}N_4O_2$: 361.1659; found: 361.1660.

4.2.23. Compound 6c

1-(5-(2-Hydroxy-phenyl)-3-(phenyl)-4,5-dihydro-pyrazol-1-yl) ethanone-2-imidazole, white powder, yield, 14%; mp 274–276 °C; ^{1}H (300 MHz, DMSO-d_6) δ (ppm): 3.06 (dd, 1H, J_1 = 4.7 Hz, J_2 = 18.0 Hz, 4-Ha), 3.82 (dd, 1H, J_1 = 11.8 Hz, J_2 = 18.0 Hz, 4-Hb), 5.31 (d, 1H, J = 17.3 Hz, Ha), 5.44 (d, 1H, J = 17.3 Hz, Hb), 5.67 (dd, 1H, J_1 = 4.6 Hz, J_2 = 11.7 Hz, 5-H), 6.85 (s, 1H, iminazole 5-H), 7.13 (s, 1H, iminazole 4-H), 7.62 (s, 1H, iminazole 2-H), 6.60–7.91 (9H, Ar-H), 9.73 (s, 1H). TOF-HRMS: m/z [M+H]$^+$ calcd for $C_{20}H_{19}N_4O_2$: 347.1503; found: 347.1503.

4.2.24. Compound 6d

1-(5-(2-Hydroxy-phenyl)-3-(4-fluoro-phenyl)-4,5-dihydro-pyrazol-1-yl)ethanone-2-imidazole, white powder, yield, 19%; mp 248–250 °C; ^{1}H (300 MHz, DMSO-d_6) δ (ppm): 3.06 (dd, 1H, J_1 = 4.7 Hz, J_2 = 18.0 Hz, 4-Ha), 3.84 (dd, 1H, J_1 = 11.7 Hz, J_2 = 18.0 Hz, 4-Hb), 5.30 (d, 1H, J = 17.3 Hz, Ha), 5.43 (d, 1H, J = 17.3 Hz, Hb), 5.67 (dd, 1H, J_1 = 4.6 Hz, J_2 = 11.7 Hz, 5-H), 6.85 (s, 1H, iminazole 5-H), 7.13 (s, 1H, iminazole 4-H), 7.62 (s, 1H, iminazole 2-H), 6.65–7.96 (8H, Ar-H), 9.73 (s, 1H). TOF-HRMS: m/z [M+H]$^+$ calcd for $C_{20}H_{18}FN_4O_2$: 365.1408; found: 365.1409.

4.2.25. Compound 6f

1-(5-(5-Chloro-2-hydroxy-phenyl)-3-(4-methoxy-phenyl)-4,5-dihydro-pyrazol-1-yl)ethanone-2-imidazole, white powder, yield, 16%; mp 231–233 °C; IR (KBr, ν/cm^{-1}): 3021 (ν_{asC-H}), 1668 ($\nu_{C=O}$), 1642 ($\nu_{C=N}$), 1457 ($\nu_{ArC=C}$), 1393 (ν_{C-H}), 1043 (ν_{C-O-C}), 831 ($\gamma_{=C-H}$), 757 ($\gamma_{=C-H}$); ^{1}H (300 MHz, DMSO-d_6) δ (ppm): 3.10 (dd, 1H, J_1 = 4.9 Hz, J_2 = 18.0 Hz, 4-Ha), 3.70–3.93 (m, 4H, CH_3O, 4-Hb), 5.26 (d, 1H, J = 17.2 Hz, Ha), 5.47 (d, 1H, J = 17.2 Hz, Hb), 5.59 (dd, 1H, J_1 = 4.8 Hz, J_2 = 11.8 Hz, 5-H), 6.85 (s, 1H, iminazole 5-H), 7.13 (s, 1H, iminazole 4-H), 7.62 (s, 1H, iminazole 2-H), 6.65–7.96 (7H, Ar-H), 10.08 (s, 1H). TOF-HRMS: m/z [M+H]$^+$ calcd for $C_{21}H_{20}ClN_4O_3$: 411.1220; found: 411.1220.

4.2.26. Compound 6g

1-(5-(5-Chloro-2-hydroxy-phenyl)-3-(4-methyl-phenyl)-4,5-dihydro-pyrazol-1-yl)ethanone-2-imidazole, white powder, yield, 20%; mp 261–263 °C; ^{1}H (300 MHz, DMSO-d_6) δ (ppm): 2.36 (s, 3H, CH_3), 3.11 (dd, 1H, J_1 = 5.0 Hz, J_2 = 18.1 Hz, 4-Ha), 3.82 (dd, 1H, J_1 = 11.7 Hz, J_2 = 18.1 Hz, 4-Hb), 5.27 (d, 1H, J = 17.2 Hz, Ha), 5.47 (d, 1H, J = 17.2 Hz, Hb), 5.60 (dd, 1H, J_1 = 5.0 Hz, J_2 = 11.8 Hz, 5-H), 6.85 (s, 1H, iminazole 5-H), 7.13 (s, 1H, iminazole 4-H), 7.62 (s, 1H, iminazole 2-H), 6.79–7.79 (7H, Ar-H), 10.10 (s, 1H). TOF-HRMS: m/z [M+H]$^+$ calcd for $C_{21}H_{20}ClN_4O_2$: 395.1269; found: 395.1269.

4.2.27. Compound 6h

1-(5-(5-Chloro-2-hydroxy-phenyl)-3-(4-fluoro-phenyl)-4,5-dihydro-pyrazol-1-yl)ethanone-2-imidazole, yellow powder, yield, 21%; mp 228–229 °C; IR (KBr, ν/cm^{-1}): 3412 (ν_{O-H}), 3115 (ν_{asCH2}), 1664 ($\nu_{C=O}$), 1602 ($\nu_{ArC=C}$), 1449 ($\nu_{ArC=C}$), 839 ($\gamma_{=C-H}$); ^{1}H (300 MHz, DMSO-d_6) δ (ppm): 3.15 (dd, 1H, J_1 = 5.1 Hz, J_2 = 18.1 Hz, 4-Ha), 3.89 (dd, 1H, J_1 = 11.9 Hz, J_2 = 18.1 Hz, 4-Hb), 5.28 (d, 1H, J = 17.2 Hz, Ha), 5.47 (d, 1H, J = 17.2 Hz, Hb), 5.61 (dd, 1H, J_1 = 5.0 Hz, J_2 = 11.9 Hz, 5-H), 6.85 (s, 1H, iminazole 5-H), 7.13 (s, 1H, iminazole 4-H), 7.62 (s, 1H, iminazole 2-H), 6.75–7.96 (7H, Ar-H), 10.09 (s, 1H); TOF-HRMS: m/z [M+H]$^+$ calcd for $C_{20}H_{17}ClFN_4O_2$: 399.1019; found: 399.1021.

4.2.28. Compound 7h

1-(5-(5-Chloro-2-hydroxy-phenyl)-3-(4-fluoro-phenyl)-4,5-dihydro-pyrazol-1-yl)ethanone-2-piperazine, white powder, yield, 11%; mp 221–223 °C; ^{1}H (300 MHz, Pyr-d_5) δ (ppm): 2.98 (s, 4H), 3.13 (s, 4H), 3.30 (dd, 1H, J_1 = 5.1 Hz, J_2 = 17.8 Hz, 4-Ha), 3.76–3.91 (m, 2H, 4-Hb, Ha), 4.13 (d, 1H, J = 15.5 Hz, Hb), 6.20 (dd, 1H, J_1 = 5.0 Hz, J_2 = 11.8 Hz, 5-H), 7.06–7.92 (7H, Ar-H), 8.85 (s, 1H); TOF-HRMS: m/z [M+H]$^+$ calcd for $C_{21}H_{23}ClFN_4O_2$: 418.1566; found: 418.1571.

4.3. General procedure for the synthesis of title compounds 11∼12

A solution of salicylaldehyde (10 mmol) and 5% NaOH aqueous solution (2 mL) in acetone (20 mL) was stirred at 40 °C for 4∼10 h until the disappearance of starting material (monitored by TLC). The mixture was allowed to cool to room temperature, neutralized with 2 M HCl to a pH in the range of 2∼3 and allowed to stand at 0 °C overnight. The resulting precipitate was collected, washed with water and dried to give compound **8**. Compound **8** was treated with 5 times excess of hydrazine hydrate in dry ethanol and refluxed for 3∼6 h. The reaction mixture was then poured into ice-cold water. The solid was filtered, washed and recrystallized from ethanol to afford respective pyrazoline (**9**). A mixture of compound **9** and bromoacetyl chloride in CH_2Cl_2 was added 4-dimethylaminopyridine (DMAP) and the reaction was stirred overnight. The reaction mixture was washed with H_2O and brine. The resulting residue was then purified by column chromatography to give compound **10**. A catalytic amount of KI was added to a acetone (20 mL) solution of compound **10** (2.0 mmol), the amine (3.0 mmol) and triethylamine (0.40 mL), then the reaction mixture was stirred at 40 °C for 10 h. The mixture was allowed to cool to room temperature and 30 mL water was added, allowed to stand at 0 °C overnight. The product was collected by filtration and the

residue was purified by chromatography on a silica gel column (petroleum/EtOAc, 1:1 → 1:3) to give title compounds **11**∼**12**.

4.3.1. Compound 11a

1-(5-(5-Chloro-2-hydroxy-phenyl)-3-methyl-4,5-dihydro-pyrazol-1-yl)ethanone-2-piperidine, yellow powder, yield, 66%; mp 151–152 °C; ^{1}H (300 MHz, $CDCl_3$) δ (ppm): 1.33–1.69 (m, 6H), 2.16 (s, 3H, CH_3), 2.45–2.60 (m, 4H), 2.92 (dd, 1H, J_1 = 3.7 Hz, J_2 = 18.6 Hz, 4-Ha), 3.33 (dd, 1H, J_1 = 11.4 Hz, J_2 = 18.6 Hz, 4-Hb), 3.52 (s, 2H, Ha, Hb), 5.60 (dd, 1H, J_1 = 3.7 Hz, J_2 = 11.4 Hz, 5-H), 6.77 (d, 1H, J = 8.6 Hz, 3′-H), 6.83 (d, 1H, J = 2.5 Hz, 4′-H), 7.06 (dd, 1H, J_1 = 2.5 Hz, J_2 = 8.6 Hz, 6′-H). TOF-HRMS: m/z [M+H]$^+$ calcd for $C_{17}H_{23}N_3O_2$: 336.1473; found: 336.1474.

4.3.2. Compound 11b

1-(5-(5-Chloro-2-hydroxy-phenyl)-3-methyl-4,5-dihydro-pyrazol-1-yl)ethanone-2-morpholin white powder, yield, 58%; mp 183–184 °C; ^{1}H (300 MHz, $CDCl_3$) δ (ppm): 2.16 (s, 3H, CH_3), 2.63 (d, 4H, J = 2.9 Hz), 2.89 (dd, 1H, J_1 = 3.6 Hz, J_2 = 18.7 Hz, 4-Ha), 3.35 (dd, 1H, J_1 = 11.4 Hz, J_2 = 18.6 Hz, 4-Hb), 3.54 (d, 1H, J = 16.7 Hz, Ha), 3.61 (d, 1H, J = 16.7 Hz, Hb), 3.77 (t, 4H, J = 4.5 Hz), 5.63 (dd, 1H, J_1 = 3.6 Hz, J_2 = 11.3 Hz, 5-H), 6.70 (d, 1H, J = 8.6 Hz, 3′-H), 6.81 (d, 1H, J = 2.5 Hz, 4′-H), 7.04 (dd, 1H, J_1 = 2.4 Hz, J_2 = 8.6 Hz, 6′-H); ^{13}C NMR (75 MHz, $CDCl_3$) δ (ppm): 16.1(CH_3), 44.2 (4-C), 54.0 (5-C, 2C), 59.5, 66.8 (2C), 119.2 (3′-C), 124.8 (5′-C), 124.9 (4′-C), 128.1(6′-C), 129.0 (1′-C), 153.3 (3-C), 158.9 (2′-C), 167.9. TOF-HRMS: m/z [M+H]$^+$ calcd for $C_{16}H_{21}ClN_3O_3$: 338.1266; found: 338.1263.

4.3.3. Compound 11c

1-(5-(5-Chloro-2-hydroxy-phenyl)-3-methyl-4,5-dihydro-pyrazol-1-yl)ethanone-2-imidazole, white powder, yield, 62%; mp 165–166 °C; IR (KBr, ν/cm^{-1}): 3418 (ν_{O-H}), 3136 ($\nu_{as=C-H}$), 2917 (ν_{asC-H}), 1678 ($\nu_{C=O}$), 1460 ($\nu_{ArC=C}$), 1431 ($\nu_{ArC=C}$), 1276, 1108, 869 ($\gamma_{=C-H}$), 820 ($\gamma_{=C-H}$); ^{1}H (300 MHz, $CDCl_3$) δ (ppm): 2.16 (s, 3H, CH_3), 2.91 (dd, 1H, J_1 = 4.4 Hz, J_2 = 18.7 Hz, 4-Ha), 3.37 (dd, 1H, J_1 = 11.2 Hz, J_2 = 18.4 Hz, 4-Hb), 5.06 (s, 2H, Ha, Hb), 5.59 (dd, 1H, J_1 = 4.5 Hz, J_2 = 11.5 Hz, 5-H), 6.74 (d, 1H, J = 8.6 Hz, 3′-H), 6.85 (d, 1H, J = 2.5 Hz, 4′-H), 6.94–7.13 (m, 3H, 6′-H, iminazole 5-H, iminazole 4-H), 7.56 (s, 1H, iminazole 2-H). TOF-HRMS: m/z [M+H]$^+$ calcd for $C_{15}H_{16}ClN_4O_2$: 319.0956; found: 319.0957.

4.3.4. Compound 12a

1-(5-(3,5-Dibromo-2-hydroxyphenyl)-3-methyl-4,5-dihydro-pyrazol-1-yl)ethanone-2-piperidine, white powder, yield, 66%; mp 186–189 °C; ^{1}H (300 MHz, $CDCl_3$) δ (ppm): 1.43–1.65 (m, 6H), 2.15 (s, 3H, CH_3), 2.51–2.64 (m, 4H), 2.88 (dd, 1H, J_1 = 3.0 Hz, J_2 = 18.8 Hz, pyrazole 4-Ha), 3.34 (dd, 1H, J_1 = 11.5 Hz, J_2 = 18.8 Hz, pyrazole 4-Hb), 3.51 (d, 1H, J = 17.0 Hz, Ha), 3.58 (d, 1H, J = 17.0 Hz, Hb), 5.58 (dd, 1H, J_1 = 3.2 Hz, J_2 = 11.2 Hz, pyrazole 5-H), 6.99 (s, 1H, 6′-H), 7.57 (s, 1H, 4′-H); ^{13}C NMR (75 MHz, $CDCl_3$) δ (ppm): 16.2 (CH_3), 24.1, 25.9, 43.9 (4-C), 54.4 (5-C), 55.1, 59.8 (CH_2C=O), 112.9 (3′-C), 114.3 (5′-C), 128.6 (6′-C), 130.6 (1′-C), 134.8 (4′-C), 151.1 (3-C), 158.1 (2′-C), 168.5 (C=O). TOF-HRMS: m/z [M+H]$^+$ calcd for $C_{17}H_{22}Br_2N_3O_2$: 458.0073; found: 458.0073.

4.3.5. Compound 12b

1-(5-(3,5-Dibromo-2-hydroxyphenyl)-3-methyl-4,5-dihydro-pyrazol-1-yl)ethanone-2-piperidin-4-one, Oil, yield, 31%; ^{1}H (300 MHz, $CDCl_3$) δ (ppm): 2.16 (s, 3H, CH_3), 2.52 (d, 4H, J = 6.0 Hz, CH_2CO), 2.84–3.02 (m, 5H, overlap, pyrazole 4-Ha, 2× CH_2), 3.37 (ddd, 1H, J_1 = 0.9 Hz, J_2 = 11.6 Hz, J_3 = 15.2 Hz, pyrazole 4-Hb), 3.65 (d, 1H, J = 16.8 Hz, Ha), 3.75 (d, 1H, J = 16.8 Hz, Hb), 5.61 (dd, 1H, J_1 = 4.2 Hz, J_2 = 11.5 Hz, pyrazole 5-H), 7.01 (d, 1H, J = 2.3 Hz, 6′-H), 7.58 (d, 1H, J = 2.3 Hz, 4′-H); ^{13}C NMR (75 MHz, $CDCl_3$) δ (ppm): 16.2 (CH_3), 41.4, 44.1 (4-C), 53.7, 54.5 (5-C), 58.2 (CH_2C=O), 113.2 (3′-C), 113.9 (5′-C), 128.7 (6′-C), 130.2 (1′-C), 134.7 (4′-C), 150.5 (3-C), 158.5 (2′-C), 168.0 (C=O), 208.9 (C=O). TOF-HRMS: m/z [M+H]$^+$ calcd for $C_{17}H_{20}Br_2N_3O_3$: 471.9866; found: 471.9862.

4.3.6. Compound 12c

1-(5-(3,5-Dibromo-2-hydroxyphenyl)-3-methyl-4,5-dihydro-pyrazol-1-yl)ethanone-2-piperazidine, colorless crystals, yield, 63%; mp 162–165 °C; IR (KBr, ν/cm^{-1}): 3425 (ν_{O-H}), 2949 (ν_{asC-H}), 2822 (ν_{sC-H}), 2720 (ν_{sC-H}), 1647 ($\nu_{C=O}$), 1457 ($\nu_{ArC=C}$), 861 ($\gamma_{=C-H}$), 702 ($\gamma_{=C-H}$); ^{1}H (300 MHz, $CDCl_3$) δ (ppm): 1.05 (t, 3H, J = 7.0 Hz, CH_3CH_2OH), 1.96 (s, 3H, CH_3C), 2.54–2.59 (m, 5H, overlap, pyrazole 4-Ha, 2× CH_2), 2.80–2.84 (m, 4H, 2× CH_2), 3.32 (m, 1H, overlap, pyrazole 4-Hb), 3.36 (d, 1H, J = 15.6 Hz, Ha), 3.44 (q, 2H, J = 7.0 Hz, CH_3CH_2OH), 3.61 (d, 1H, J = 15.8 Hz, Hb), 5.43 (dd, 1H, J_1 = 4.6 Hz, J_2 = 11.5 Hz, pyrazole 5-H), 6.76 (d, 1H, J = 2.4 Hz, 6′-H), 7.43 (d, 1H, J = 2.4 Hz, 4′-H); ^{13}C NMR (75 MHz, $CDCl_3$) δ (ppm): 15.6 (CH_3), 18.4, 44.1 (4-C), 44.2, 51.7, 55.8 (5-C), 56.0, 58.6 (CH_2C=O), 105.1 (3′-C), 113.6 (5′-C), 127.1 (6′-C), 132.2 (1′-C), 132.7 (4′-C), 155.4 (3-C), 157.4 (2′-C), 165.8 (C=O). TOF-HRMS: m/z [M+H]$^+$ calcd for $C_{16}H_{21}Br_2N_4O_2$: 459.0026; found: 459.0023.

4.3.7. Compound 12d

1-(5-(3,5-Dibromo-2-hydroxyphenyl)-3-methyl-4,5-dihydro-pyrazol-1-yl)ethanone-2-(4-hydroxyethyl)piperazidine, white powder, yield, 72%; mp 236–238 °C; ^{1}H (300 MHz, C_5D_5N) δ (ppm): 1.96 (s, 3H, CH_3), 2.64–2.85 (m, 11H, 5× CH_2, pyrazole 4-Ha), 3.37 (dd, 1H, J_1 = 11.6 Hz, J_2 = 18.1 Hz, pyrazole 4-Hb), 3.68 (d, 1H, J = 15.2 Hz, Ha), 3.92 (d, 2H, J = 6.3 Hz, CH_2OH), 3.92 (d, 1H, J = 14.8 Hz, Hb), 5.99 (dd, 1H, J_1 = 4.8 Hz, J_2 = 11.5 Hz, pyrazole 5-H), 7.47 (s, 1H, 6′-H), 7.72 (s, 1H, 4′-H); ^{13}C NMR (75 MHz, C_5D_5N) δ (ppm): 16.0 (CH_3), 44.9 (4-C), 54.2, 54.3, 56.5 (5-C), 59.8, 60.0 (CH_2C=O), 61.7 (CH_2OH), 112.7 (3′-C), 114.1 (5′-C), 129.1 (6′-C), 134.4 (1′-C), 134.8 (4′-C), 152.3 (3-C), 157.3 (2′-C), 167.9 (C=O). TOF-HRMS: m/z [M+H]$^+$ calcd for $C_{18}H_{25}Br_2N_4O_3$: 503.0288; found: 503.0287.

4.3.8. Compound 12e

1-(5-(3,5-Dibromo-2-hydroxyphenyl)-3-methyl-4,5-dihydro-pyrazol-1-yl)ethanone-2-(4-hydroxyl)piperidine, colorless crystals, yield, 48%; mp 89–92 °C; ^{1}H (300 MHz, $CDCl_3$) δ (ppm): 1.61–1.74 (m, 2H), 1.90–1.99 (m, 2H), 2.15 (s, 3H, CH_3), 2.39–2.50 (m, 2H), 2.87 (dd, 1H, J_1 = 4.2 Hz, J_2 = 15.8 Hz, pyrazole 4-Ha), 2.88–3.00 (m, 2H), 3.35 (dd, 1H, J_1 = 11.6 Hz, J_2 = 15.8 Hz, pyrazole 4-Hb), 3.56 (d, 1H, J = 16.7 Hz, Ha), 3.64 (d, 1H, J = 16.7 Hz, Hb), 3.69–3.79 (m, 1H), 5.59 (dd, 1H, J_1 = 4.2 Hz, J_2 = 11.5 Hz, pyrazole 5-H), 6.99 (d, 1H, J = 2.3 Hz, 6′-H), 7.57 (d, 1H, J = 2.3 Hz, 4′-H); ^{13}C NMR (75 MHz, $CDCl_3$) δ (ppm): 16.2 (CH_3), 34.2, 44.1 (4-C), 51.5, 54.6 (5-C), 58.8 (CH_2C=O), 67.4 (CH_2-OH), 113.0 (3′-C), 114.1 (5′-C), 128.7 (6′-C), 130.6 (1′-C), 134.7 (4′-C), 150.8 (3-C), 158.3 (2′-C), 168.0 (C=O). TOF-HRMS: m/z [M+H]$^+$ calcd for $C_{17}H_{22}Br_2N_3O_3$: 474.0022; found: 474.0019.

4.3.9. Compound 12f

1-(5-(3,5-Dibromo-2-hydroxyphenyl)-3-methyl-4,5-dihydro-pyrazol-1-yl)ethanone-2-(4-hydroxymethyl)piperidine, colorless crystals, yield, 65%; mp 215–217 °C; IR (KBr, ν/cm^{-1}): 3416 (ν_{O-H}), 2929 (ν_{asCH2}), 2850 (ν_{sCH2}), 1635 ($\nu_{C=O}$), 1461 ($\nu_{ArC=C}$), 866 ($\gamma_{=C-H}$); ^{1}H (300 MHz, DMSO-d_6) δ (ppm): 1.15–1.34 (m, 3H), 1.57–1.61 (m, 2H), 1.98 (s, 3H, CH_3), 2.02–2.16 (m, 2H), 2.58 (dd, 1H, J_1 = 4.7 Hz, J_2 = 18.5 Hz, pyrazole 4-Ha), 2.84–2.93 (m, 2H), 3.22 (d, 2H, J = 6.2 Hz, CH_2OH), 3.31 (d, 1H, J = 15.5 Hz, Ha), 3.40 (dd, 1H, J_1 = 11.7 Hz, J_2 = 18.6 Hz, pyrazole 4-Hb), 3.62 (d, 1H, J = 15.5 Hz, Hb), 5.49 (dd, 1H, J_1 = 4.7 Hz, J_2 = 11.6 Hz, pyrazole 5-H), 6.90 (d, 1H, J = 2.3 Hz, 6′-H), 7.62 (d, 1H, J = 2.4 Hz, 4′-H); ^{13}C NMR (75 MHz, DMSO-d_6) δ (ppm): 15.5 (CH_3), 28.5 (CH_2), 28.6 (CH_2),

37.9 (CH), 44.1 (4-C), 53.1, 53.2, 54.7 (5-C), 58.9 (CH_2C=O), 66.0 (CH_2OH), 111.1 (3′-C), 112.6 (5′-C), 127.4 (6′-C), 132.9 (1′-C), 133.0 (4′-C), 150.2 (3-C), 157.2 (2′-C), 166.4 (C=O). TOF-HRMS: m/z $[M+H]^+$ calcd for $C_{18}H_{24}Br_2N_3O_3$: 488.0179; found: 488.0175.

4.4. Crystallographic studies

X-ray single-crystal diffraction data for compounds **4f**, **12c** and **12f** was collected on a Bruker SMART APEX CCD diffractometer at 293(2) K using MoKα radiation (λ = 0.71073 Å) by the ω scan mode. The program SAINT was used for integration of the diffraction profiles. The structure was solved by direct methods using the SHELXS program of the SHELXTL package and refined by full-matrix least-squares methods with SHELXL.[21] The corrections for *LP* factors were applied. All non-hydrogen atoms of compounds **4f**, **12c** and **12f** were refined with anisotropic thermal parameters. All hydrogen atoms were generated theoretically onto the parent atoms and refined isotropically with fixed thermal factors.

4.5. hMAO activity assay

Enzymatic MAO-A and MAO-B activity of compounds was determined by a fluorimetric method.[22] Briefly, 0.1 mL of sodium phosphate buffer (0.05 M, pH 7.4) containing various concentrations of the test drugs (new compounds or reference inhibitors). The appropriate amounts of recombinant hMAO-A or hMAO-B was adjusted to the same reaction velocity in the presence of both isoforms the same concentration of substrate: 165 pmol of *p*-tyramine/min (hMAO-A: 1.1 μg protein; specific activity: 150 nmol of *p*-tyramine oxidized top hydroxy phenylacetaldehyde/min/mg protein; hMAO-B: 7.5 μg protein; specific activity: 22 nmol of *p*-tyramine transformed/min/mg protein). The mixture was incubated for 15 min at 37 °C, placed in the dark fluorimeter chamber. After this incubation period, the reaction was started by adding 200 μM of 10-acetyl-3,7-dihydroxyphenoxazine reagent (Amplex Red assay kit, Molecular Probes, Inc., Eugene, OR), 1 U/mL horseradish peroxidase, and 1 mM *p*-tyramine. The production of H_2O_2 and, consequently, of resorufin, was quantified at 37 °C in a multidetection microplate fluorescence reader based on the fluorescence generated (excitation, 545 nm, emission, 590 nm) over a 15 min period, during which the fluorescence increased linearly.

4.6. General procedure for molecular docking

Discovery studio 3.1 (DS 3.1, Accelrys Software Inc., San Diego, California, USA). Crystal structure of hMAO-A (2BXR pdb) was used as template. Hydrogen atoms were added to protein model. The added hydrogen atoms were minimized to have stable energy conformation and to also relax the conformation from close contacts. The active site was defined and sphere of 4 Å was generated around the active site pocket, with the active site pocket of BSAI model using C-DOCKER, a molecular dynamics (MD) simulated-annealing based algorithm module from DS 3.1 Random substrate conformations are generated using high-temperature MD. The whole 2BXR was defined as a receptor, and the site sphere was selected based on the active centre of 2BXR according to a previous report.[25] Candidate poses are then created using random rigid-body rotations followed by simulated annealing. The structure of protein, substrate were subjected to energy minimization using CHARMm forcefield as implemented in DS 3.1. A full potential final minimization was then used to refine the substrate poses. Based on CDOCKER, energy docked conformation of the substrate was retrieved for postdocking analysis.

5. Supporting information

Crystallographic data (excluding structure factors) for the structure had been deposited with the Cambridge Crystallographic Data Center as supplementary publication No. CCDC 1021033 (**4f**), CCDC 976177 (**12c**) and CCDC 976176 (**12f**). These data can be obtained free of charge via the URL http:// www.ccdc.cam.ac.uk/conts/retrieving.html (or from the CCDC, 12 Union Road, Cambridge CB2 1EZ, UK; fax: (+44) 1223 336033; e-mail: deposit@ccdc.cam.ac.uk). Representative ^{1}H and ^{13}C NMR spectra (containing **4a**∼**4g**, **4i**, **5a**∼**5c**, **5e**, **5h**, **5i**, **6a**, **11b**, **12a**∼**12f**).

Acknowledgments

The authors wish to thank the National Natural Science Foundation of China (Nos. 21272008, 20802003), Science and Technological Fund of Anhui Province for Outstanding Youth, China (1408085J04), National Training Programs of Innovation and Entrepreneurship for Undergraduates (201410366041), China.

Supplementary data

Supplementary data associated with this article can be found, in the online version, at http://dx.doi.org/10.1016/j.bmc.2014.12.010.

References and notes

1. Binda, C.; Wang, J.; Pisani, L.; Caccia, C.; Carotti, A.; Salvati, P.; Edmondson, D. E.; Mattevi, A. *J. Med. Chem.* **2007**, *50*, 5848.
2. Edmondson, D. E.; Binda, C.; Mattevi, A. *Arch. Biochem. Biophys.* **2007**, *464*, 269.
3. De Colibus, L.; Li, M.; Binda, C.; Lustig, A.; Edmondson, D. E.; Mattevi, A. *Proc. Natl. Acad. Sci. U.S.A.* **2005**, *102*, 12684.
4. Binda, C.; Newton-Vinson, P.; Hubálek, F.; Edmonson, D. E.; Mattevi, A. *Nat. Struct. Biol.* **2002**, *9*, 22.
5. Son, S. Y.; Ma, J.; Kondou, Y.; Yoshimura, M.; Yamashita, E.; Tsukihara, T. *Proc. Natl. Acad. Sci. U.S.A.* **2008**, *105*, 5739.
6. Ma, J.; Yoshimura, M.; Yamashita, E.; Nakagawa, A.; Ito, A.; Tsukihara, T. *J. Mol. Biol.* **2004**, *338*, 103.
7. Naoi, M.; Maruyama, W.; Inaba-Hasegawa, K. *Curr. Top. Med. Chem.* **2012**, *12*, 2177.
8. Riederer, P.; Lachenmayer, L.; Laux, G. *Curr. Med. Chem.* **2004**, *11*, 2033.
9. Secci, D.; Bolasco, A.; Chimenti, P.; Carradori, S. *Curr. Med. Chem.* **2011**, *18*, 5114.
10. Secci, D.; Carradori, S.; Bolasco, A.; Bizzarri, B.; D'Ascenzio, M.; Maccioni, E. *Curr. Top. Med. Chem.* **2012**, *12*, 2240.
11. Chimenti, F.; Bolasco, A.; Manna, F.; Secci, D.; Chimenti, P.; Granese, A.; Befani, O.; Turini, P.; Cirilli, R.; La Torre, F.; Alcaro, S.; Ortuso, F.; Langer, T. *Curr. Med. Chem.* **2006**, *13*, 1411.
12. Jagrat, M.; Behera, J.; Yabanoglu, S.; Ercan, A.; Ucar, G.; Sinha, B. N.; Sankaran, V.; Basu, A.; Jayaprakash, V. *Bioorg. Med. Chem. Lett.* **2011**, *21*, 4296.
13. Kaplancıklı, Z. A.; Özdemir, A.; Turan-Zitouni, G.; Altıntop, M. D.; Can, O. D. *Eur. J. Med. Chem.* **2010**, *45*, 4383.
14. Karuppasamy, M.; Mahapatra, M.; Yabanoglu, S.; Ucar, G.; Sinha, B. N.; Basu, A.; Mishra, N.; Sharon, A.; Kulandaivelu, U.; Jayaprakash, V. *Bioorg. Med. Chem.* **1875**, *2010*, 18.
15. Salgın-Gökşen, U.; Yabanoğlu-Çiftçi, S.; Ercan, A.; Yelekçi, K.; Uçar, G.; Gökhan-Kelekçi, N. J. *Neural. Transm.* **2013**, *120*, 863.
16. Palaska, E.; Aytemir, M.; Uzbay, I. T.; Erol, D. *Eur. J. Med. Chem.* **2001**, *36*, 539.
17. Can, Ö. D.; Özkay, Ü. D.; Kaplancıklı, Z. A.; Öztürk, Y. *Arch. Pharm. Res.* **2009**, *32*, 1293.
18. Feixas, F.; Lindert, S.; Sinko, W.; McCammon, J. A. *Biophy. Chem.* **2014**, *186*, 31.
19. Dawey, W.; Tivey, D. J. *J. Chem. Soc.* **1958**, *242*, 1230.
20. Liu, X. H.; Li, J.; Shi, J. B.; Song, B. A.; Qi, X. B. *Eur. J. Med. Chem.* **2012**, *51*, 294.
21. Sheldrick, G. M. *SHELXTL-97, Program for Crystal Structure Solution and Refinement*; University of Göttingen: Göttingen, Germany, 1997.
22. Santana, L.; González-Díáz, H.; Quezada, E.; Uriarte, E.; Yañez, M.; Viña, D.; Orallo, F. *J. Med. Chem.* **2008**, *51*, 6740.
23. Chimenti, F.; Bolasco, A.; Manna, F.; Secci, D.; Chimenti, P.; Befani, O.; Turini, P.; Giovannini, V.; Mondovi, B.; Cirilli, R.; La Torre, F. *J. Med. Chem.* **2004**, *47*, 2071.
24. Milczek, E. M.; Bonivento, D.; Binda, C.; Mattevi, A.; McDonald, I. A.; Edmondson, D. E. *J. Med. Chem.* **2008**, *51*, 8019.
25. Pan, Z. X.; He, X.; Chen, Y. Y.; Tang, W. J.; Shi, J. B.; Tang, Y. L.; Song, B. A.; Liu, X. H. *Eur. J. Med. Chem.* **2014**, *80*, 278.